Structural Engineering and Mechanics, Vol. 27, No. 4 (2007) 393-408
DOI: http://dx.doi.org/10.12989/sem.2007.27.4.393

Effectiveness of CFRP-jackets in post-earthquake and pre-earthquake retrofitting of beam-column subassemblages

Alexander G. Tsonos†

Aristotle University of Thessaloniki, School of Engineering, 541 24 Thessaloniki, Greece

(Received February 14, 2006, Accepted April 25, 2007)

Abstract. This paper presents the findings of an experimental study to evaluate retrofit methods which address particular weaknesses that are often found in reinforced concrete structures, especially older structures, namely the lack of the required flexural and shear reinforcement within the columns and the lack of the required shear reinforcement within the joints. Thus, the use of a high-strength fiber jacket for cases of post-earthquake and pre-earthquake retrofitting of columns and beam-column joints was investigated experimentally. In this paper, the effectiveness of the two jacket styles was also compared.

Keywords: evaluation and retrofit; buildings; structural response concrete; composite materials; cement grout.

1. Introduction

Damage caused by earthquakes over the years, has indicated that some reinforced concrete buildings designed and constructed in the 1960's and 1970's were found to have serious structural deficiencies. These deficiencies are mainly a consequence of a lack of capacity design approach and/or poor detailing of reinforcement. As a result, lateral strength and ductility of these structures were minimal (Hakuto *et al*. 2000, Penelis and Kappos 1997, Karayannis *et al*. 1998, Dritsos 2001, Dritsos 2005). The wrapping of reinforced concrete members with fiber-reinforced polymer (FRP) sheets including carbon (C), glass (G), or aramid (A) fibers, bonded together in a matrix made of epoxy, vinylester or polyester, has been used extensively throughout the world in numerous retrofit applications in reinforced concrete buildings. These are recognized as alternate strengthening systems to conventional methods, such as steel plate bonding and shotcreting (ACI Committee 440R-96, Antonopoulos and Triantafillou 2003, Dritsos 1997, Ilki and Kumbasar 2002, Priestley *et al*. 1996, FIB 2001, Thermou and Elnashai 2006, Tsonos *et al*. 2002).

The feasibility and technical effectiveness of the high-strength fiber jacket system both in a post-earthquake and pre-earthquake retrofitting case of columns and beam-column joints was investigated and presented in this paper. Thus, two identical reinforced concrete exterior beam-column-slab-transverse beam subassemblages (F_1 and S_1) were constructed with non-optimal design parameters such as flexural strength ratio or joint shear stress, with less column transverse reinforcement than

† Professor, E-mail: tsonosa@civil.auth.gr

that required by the modern Codes (Greek Code for the Design of Reinforced Concrete Structures - C.D.C.S.-2000, Eurocode 2-2003, and Eurocode 8-2004) and without joint transverse reinforcement, representing the common construction practice of column and beam-column joints in older structures built in the 1960's and 1970's.

The subassemblage F_1 was subjected to cyclic lateral load histories so as to provide the equivalent of severe earthquake damage. The damaged specimen was then strengthened by high-strength fiber jacket. This jacket was applied in the columns and *b/c* joint regions of the damaged subassemblage F_1. The subassemblage S_1 represents part of an old frame structure, which was upgraded to resist strong future earthquakes. This subassemblage was tested only after strengthening by high-strength fiber-jacket. This jacket was also applied in the columns and *b/c* joint regions of the subassemblage S_1. The two repaired and strengthened subassemblages were subjected to cyclic lateral load history so as to provide the equivalent of severe earthquake damage.

A direct comparison of the load deflection envelopes of the original and the retrofitted subassemblages was provided in the paper. The effectiveness of the two jacket styles was also compared.

2. Description of the specimens

2.1 Original test specimens F_1 and S_1

Two identical test specimens F_1 and S_1 were constructed using normal weight concrete and deformed reinforcement. Both specimens were typical of existing older structures built in the 1960's and 1970's. In "Recommendations for Design of Beam-Column Joints in Monolithic Reinforced Concrete Structures (ACI 352R-02)", the ACI-ASCE Committee specifies the maximum allowable joint shear stresses in the form of $\gamma\sqrt{f_c'}$ MPa, where joint shear stress factor γ is a function of the joint type (i.e., interior, exterior, and so on) and of the severity of the loading, and f_c' is the concrete's compressive strength. The lower limits of the flexural strength ratio M_R and joint transverse reinforcement are also specified by the Committee. Thus, for the beam-column connections examined in this investigation, the lower limits of M_R and γ are 1.40 and 1.00 respectively.

In Fig. 1 the dimensions and cross-sectional details of specimens F_1 and S_1 are shown. Both specimens had less column transverse reinforcement than that required by the new Greek Code for the Design of Reinforced Concrete Structures (C.D.C.S.-2000) or by Eurocode 2-2003 and Eurocode 8-2004. In addition, these specimens did not have any joint transverse reinforcement (often ties in the joint region were simply omitted in the construction process in the past because of the extreme difficulty they created in the placing of reinforcement), whereas the values of flexural strength ratio were less than 1.40, and those of the joint shear stress were greater than $1.0\sqrt{f_c'}$ MPa for both specimens F_1 and S_1 (see Table 1). Thus, the beam-column connection of the original specimens could be expected to fail in shear. The dimensions of the test specimens were primarily dictated by the availability of formwork and laboratory testing capacities, resulting in a beam-to-column subassemblage model of approximately 1:2 scale. The concrete compressive strengths of specimens F_1 and S_1 were 22.00 MPa and 21.80 MPa respectively. Approximately 10 electrical-resistance strain gages were bonded in the reinforcing bars of each specimen F_1 and S_1.

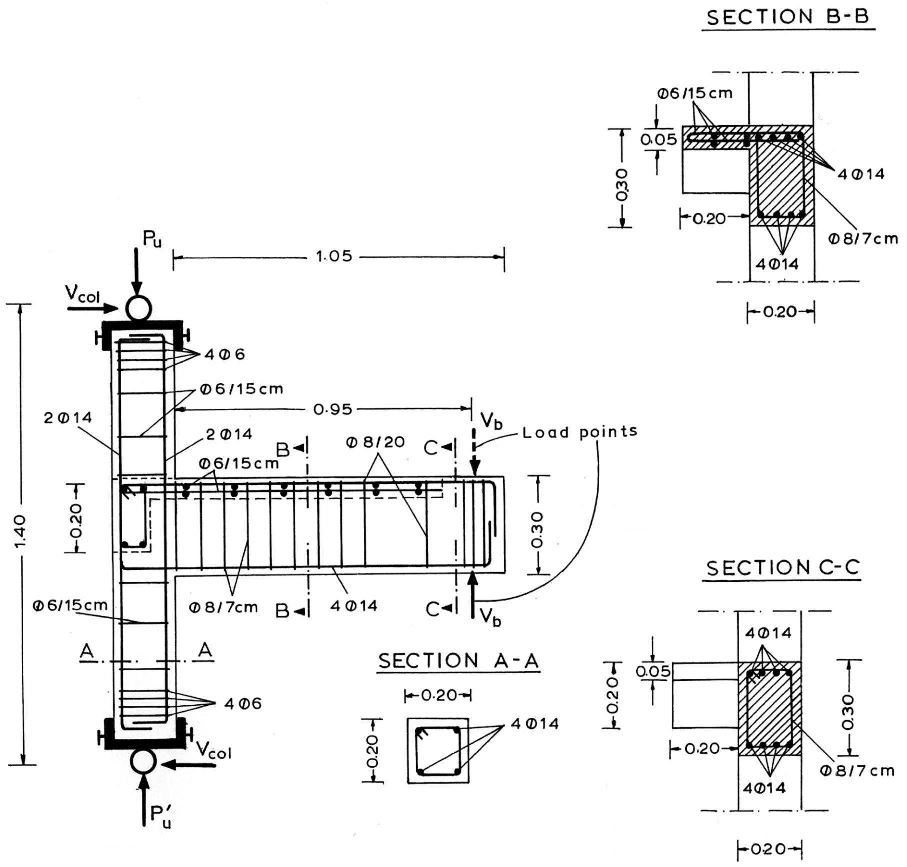

Fig. 1 Dimensions and cross-sectional details of original specimens F_1 and S_1 (dimensions in *m*)

Table 1 Flexural strength ratio M_R and the joint shear stresses factor γ of subassemblages F_1, $FRPF_1$ and $FRPS_1$

Specimen	$M_R^{(1)}$	$\gamma^{(1)}$
F_1	0.95 (1.40)	1.70 (1.00)
S_1	0.95 (1.40)	1.70 (1.00)
$FRPF_1$	1.95 (1.40)	1.70 (1.00)
$FRPS_1$	1.95 (1.40)	1.70 (1.00)

(1)Numbers outside the parentheses are the provided values, numbers inside the parentheses are the required values by the *ACI-ASCE Committee 352-02*.

2.2 Strengthening technique: Specimens $FRPF_1$ and $FRPS_1$

The original specimen F_1 had experienced brittle shear failure at the joint region.

The repair measures implemented on specimen F_1 consisted of: (1) the removal and replacement of all loose concrete by a premixed, non-shrink, rheoplastic, flowable and non-segregating mortar of high-strength, and (2) a high-strength fiber jacketing in the joint region and on the columns, see

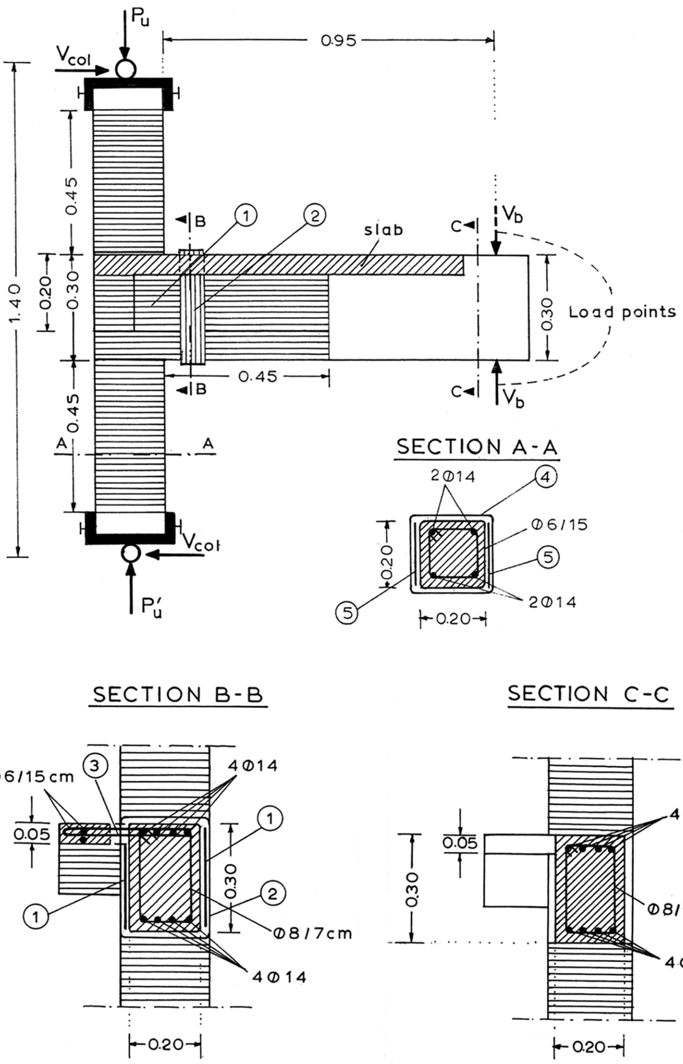

① **10 layers of CFRPs for increasing the shear strength of the joint**

② **Strips of CFRPs to secure the anchorage length of the joint layers**

③ **Drilled holes in the slabs of specimens $FRPF_1$ and $FRPS_1$**

④ **7 layers of CFRPs for increasing the shear strength of the columns**

⑤ **9 layers of CFRPs for increasing the flexural strength of the columns**

Fig. 2 Jacketing of column and beam-column connection of subassemblages $FRPF_1$ and $FRPS_1$ (dimensions in *m*)

Fig. 2. The repaired and strengthened specimen was designated $FRPF_1$. The design for the retrofit with carbon fiber-reinforced polymer sheets (CFRPs) was based on $E_f = 230$ GPa, $t_f = 0.165$ mm (t_f = layer thickness) and $\varepsilon_{fu} = 1.5\%$ (ε_{fu} = ultimate FRP strain).

The subassemblage S_1 represent part of an old frame structure which was upgraded to resist strong future earthquakes. So the specimen S_1 was tested after strengthening by high-strength fiber

Table 2 Original and strengthened specimens' steel yield stress

Bar diameter	Steel yield stress (MPa)
Ø6	560
Ø8	605
Ø14	540

jacketing as specimen $FRPS_1$. The strengthening scheme of specimen $FRPS_1$ was the same as that of specimen $FRPF_1$ (Fig. 2). However, it is obvious that the strengthening scheme of specimen $FRPS_1$ does not include the removal and replacement of the loose concrete in the joint region with a premixed, high-strength mortar, as was included in the strengthening scheme for specimen $FRPF_1$.

The original specimen F_1, S_1, were constructed using deformed reinforcement (NOTE: Ø6, Ø8, Ø14 = bar with diameter 6 mm, 8 mm, 14 mm respectively). The subassemblages steel yield stresses are shown in Table 2. Approximately 10 electrical-resistance strain gages were bonded in the reinforcing bars of each strengthened subassemblage $FRPF_1$ and $FRPS_1$.

Due to length limitations all the computations related to the strengthening of specimens $FRPF_1$ and $FRPS_1$ are in Reference Tsonos 2003 and are not incorporated in this paper.

3. Test setup-loading sequence

The general arrangement of the experimental set-up is shown in Fig. 3(a). All specimens F_1, $FRPF_1$ and $FRPS_1$ were subjected to several cycles applied by slowly displacing the beam's free end, according to the load history shown in Fig. 3(b) without reaching the actuator stroke limit. The

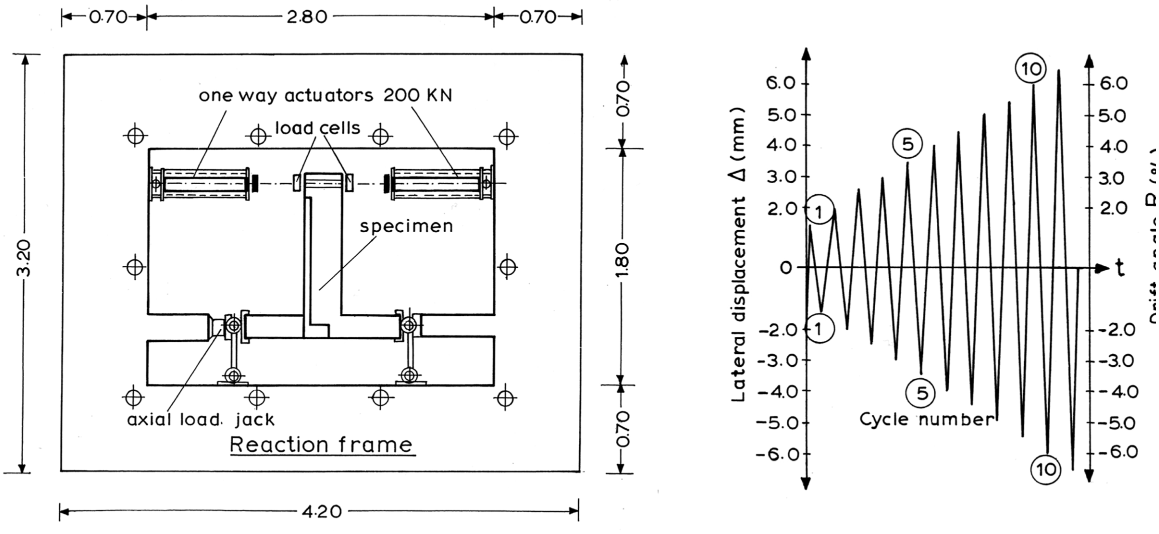

(a) (b)

Fig. 3 (a) Test setup (dimensions in mm), (b) Lateral displacement history amplitudes of the peaks in the displacement history were 15 mm, 20 mm, 25 mm, 30 mm, 35 mm, 40 mm, 45 mm, 50 mm, 55 mm, 60 mm and 65 mm. One loading cycle was performed at each displacement amplitude. An axial load equal to 150 kN was applied to the columns of the subassemblages F_1, $FRPF_1$ and $FRPS_1$ and kept constant throughout the test. As previously mentioned, all the specimens were loaded slowly. The strain rate of the load applied corresponded to static conditions.

4. Test results

The connections of the original subassemblage F_1 exhibited , as expected, premature shear failure during the early stages of cyclic loading. Damage occurred both in the joint area and in the critical regions of the columns. The beam in the specimen F_1 remained intact at the conclusion of the tests (Fig. 4(a)). The failure mode of specimens $FRPF_1$ and $FRPS_1$ involved, as expected, the formation of a plastic hinge in the beam near the column juncture, and more damage concentration in this region, but there was also little damage in the joint with partial loss of joint concrete cover. Views of the collapsed subassemblages F_1, $FRPF_1$ and $FRPS_1$ are shown in Fig. 4(a). In order to detect the failure modes of subassemblages $FRPF_1$ and $FRPS_1$, the strengthening layers of FRPs in both beams and beam-column joints were cut and subsequently removed. Thus, Fig. 4(b) reveals the damage

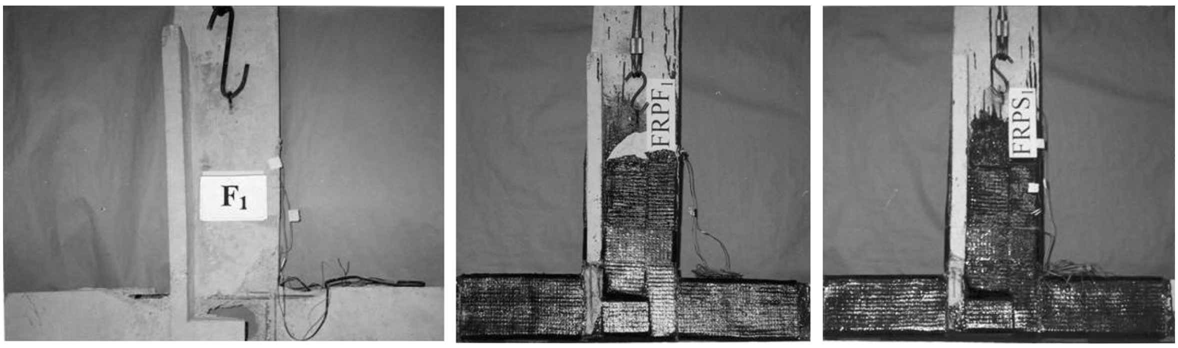

(a)

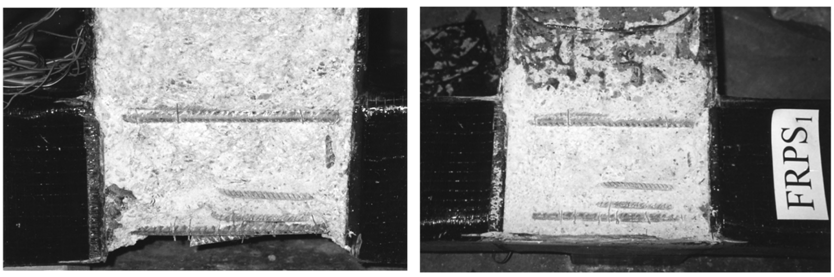

specimen $FRPF_1$ specimen $FRPS_1$

(b)

Fig. 4 (a) Views of the collapsed subassemblages: F_1, $FRPF_1$ and $FRPS_1$, (b) Post-damage views of the collapsed subassemblages $FRPF_1$ and $FRPS_1$ following removal of the reinforcing sheets

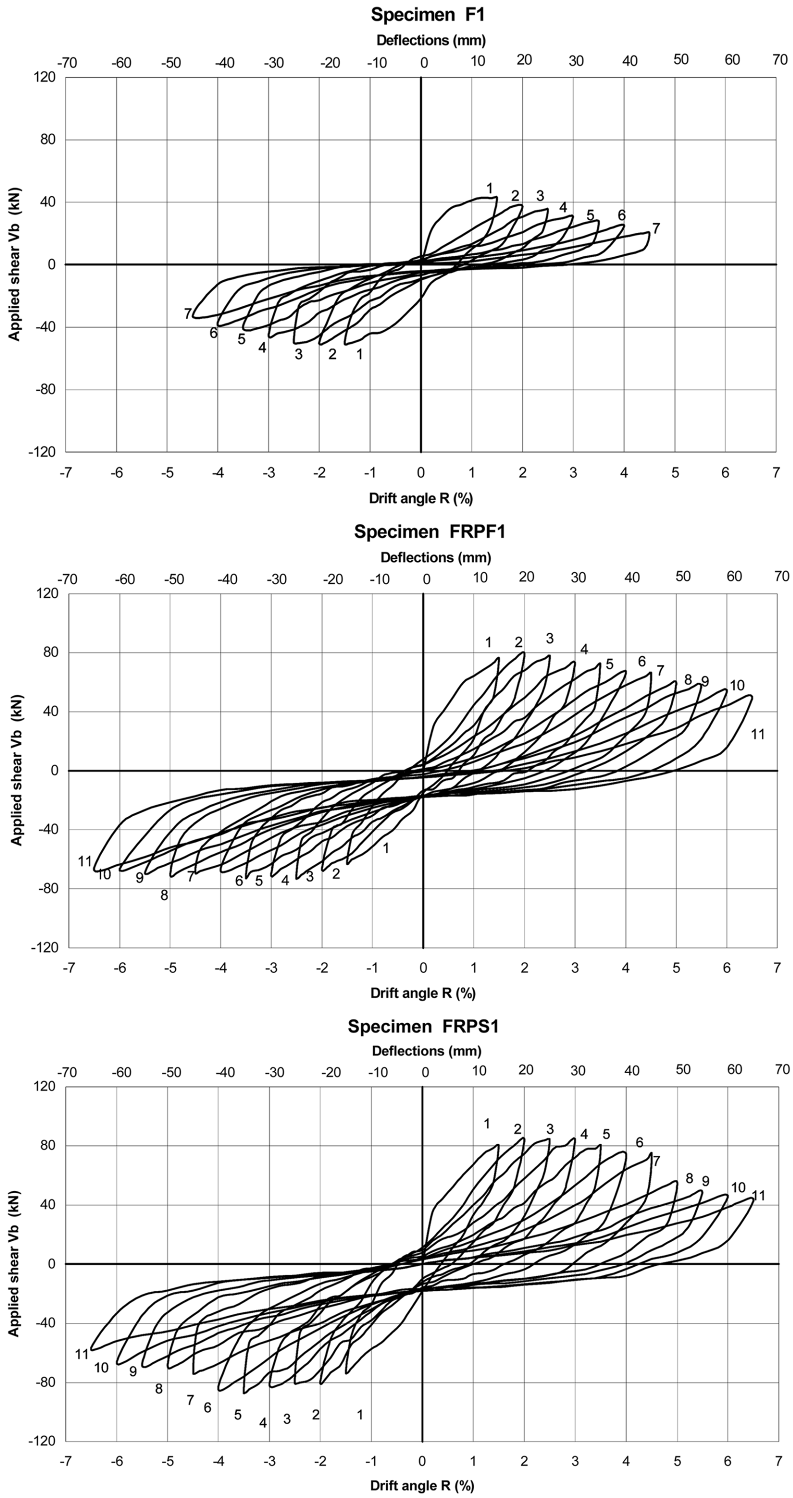

Fig. 5 Plots of applied shear-versus-drift angle for specimens F_1, $FRPF_1$ and $FRPS_1$

pattern that developed in subassemblages $FRPF_1$ and $FRPS_1$.

Plots of applied shear-versus-drift angle for all the specimens F_1, $FRPF_1$ and $FRPS_1$ are shown in Fig. 5. Subassemblages $FRPF_1$ and $FRPS_1$, strengthened with CFRP layers exhibited stable hysteresis up to the 5th cycle of drift angle R of 3.5 percent and up to the 6th cycle of drift angle R of 4.0 percent, respectively. Specimen $FRPS_1$ showed a considerable loss of strength, stiffness and unstable degrading hysteresis beyond drift angle R ratios of 4 percent while specimen $FRPF_1$ did not show any unstable degrading hysteresis (Fig. 5).

In order to study the effectiveness of fiber carbon/epoxy jacketing in improving the earthquake resistance of columns and beam-column joints in a post-earthquake strengthening case, the seismic behavior of the strengthened specimen $FRPF_1$ was compared to that of the original one F_1. On the other hand, as the original specimen S_1 had not been subjected to any cyclic loading before strengthening, in order to study the effectiveness of the jackets in a pre-earthquake strengthening case, it was decided to compare the seismic behavior of the strengthened specimen $FRPS_1$ with that of the original one F_1. Figs. 6 and 7 summarize the comparisons of the seismic behavior of the strengthened specimens $FRPF_1$ and $FRPS_1$ with that of the original one F_1 respectively (specimen S_1 is similar to specimen F_1, see Fig. 1). As comparison parameters have been chosen the most critical ones with regard to the seismic behavior of a R/C substructure such as stiffness, energy dissipation

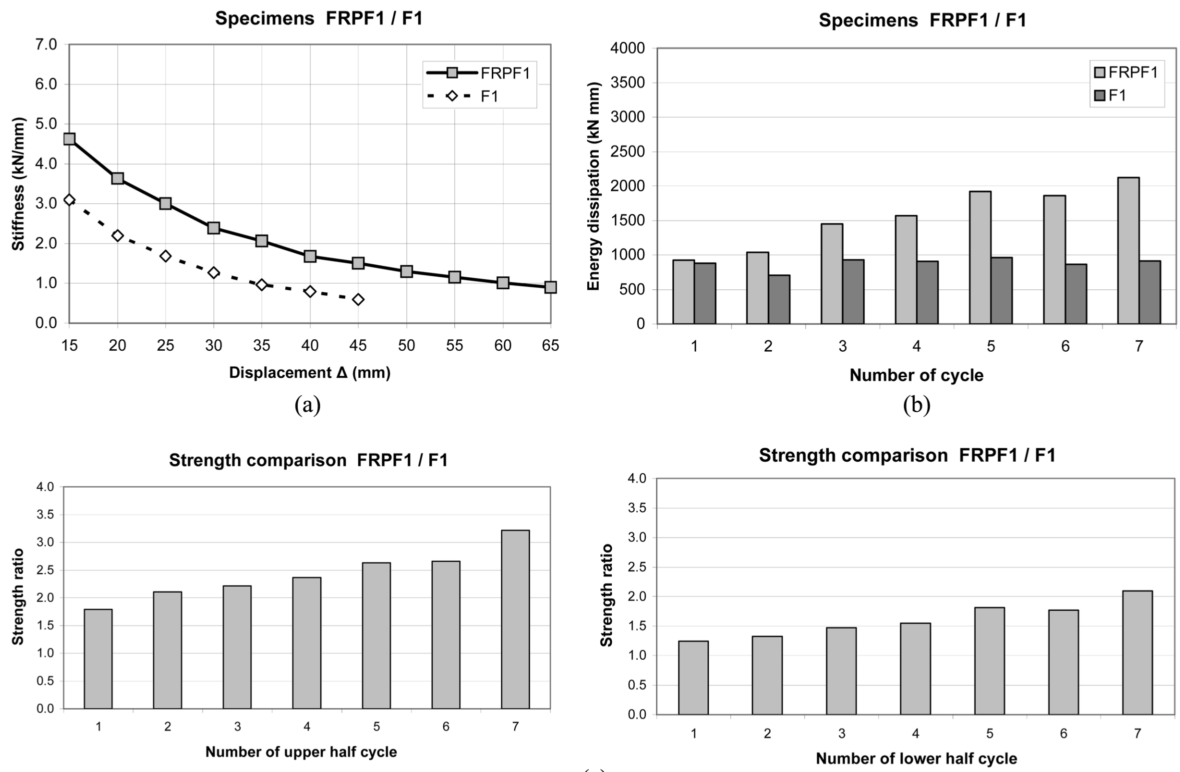

(a) (b) (c)

Fig. 6 Comparisons of the strengthened specimen $FRPF_1$ to the original one F_1: (a) Stiffness comparison, (b) Energy dissipation comparison, (c) Strength comparison

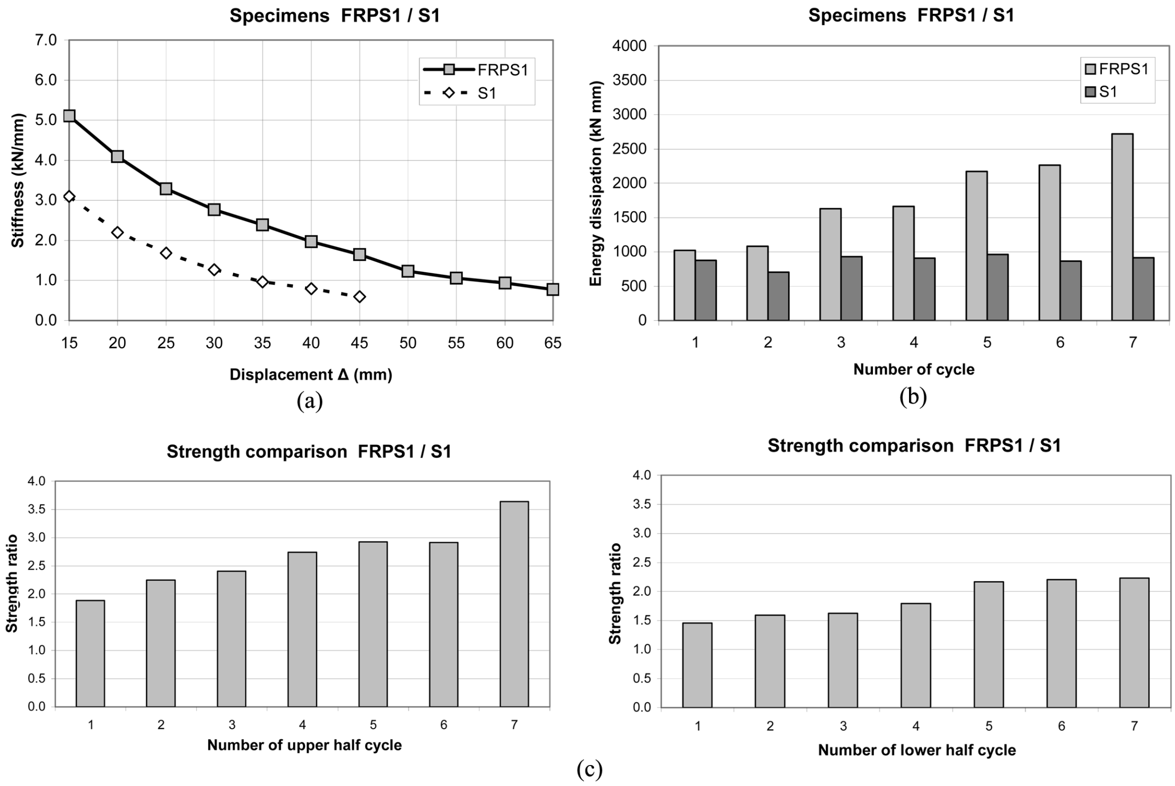

Fig. 7 Comparisons of the strengthened specimen $FRPS_1$ to the original one S_1: (a) Stiffness comparison, (b) Energy dissipation comparison, (c) Strength comparison

capacity and strength. Figs. 6 to 7 show comparisons of the peak-to-peak stiffness (Fig. 6(a) to 7(a)), energy dissipation capacity (Fig. 6(b) to 7(b)) and peak strength (Fig. 6(c) to 7(c)) observed for every load cycle of the referred specimens.

Specimen $FRPF_1$ showed up to 50% higher stiffness, up to 135% higher energy dissipation capacity and up to 170% higher strength than specimen F_1 (Fig. 6). Subassemblage $FRPS_1$ demonstrated up to 70% higher stiffness, up to 200% higher energy dissipation capacity and up to 190% higher strength than subassemblage F_1 (Fig. 7).

To compare the effectiveness between the pre-earthquake and post-earthquake type of strengthening it is interesting to compare the strength, stiffness and energy dissipation capacity between specimens $FRPS_1$ and $FRPF_1$ (Fig. 8).

From the diagrams of Fig. 8 it is clearly seen that the seismic performance of specimen $FRPS_1$ strengthened in a pre-earthquake case was better than that of specimen $FRPF_1$ strengthened in a post-earthquake case. Thus, subassemblage $FRPS_1$ shows up to 10% higher stiffness (Fig. 8(a)), up to 30% more energy dissipated (Fig. 8(b)) and up to 20% higher strength (Fig. 8(c)) than subassemblage $FRPF_1$.

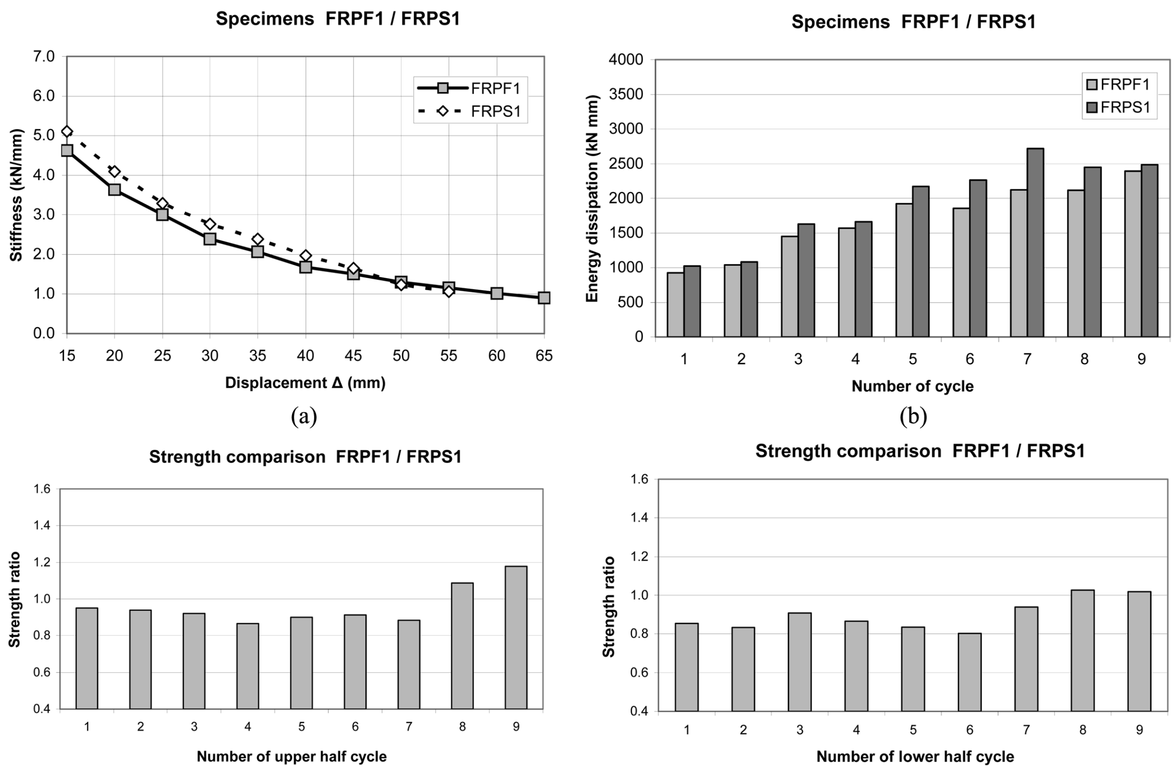

(c)

Fig. 8 Comparisons between the strengthened specimens $FRPF_1$ and $FRPS_1$: (a) Stiffness comparison, (b) Energy dissipation comparison, (c) Strength comparison

5. Theoretical considerations

5.1 Specimens strengthened by high-strength fiber jackets ($FRPF_1$ and $FRPS_1$)

The shear capacities of the strengthened columns and beam-column joints can be calculated as follows

$$V_{Rd} = V_{cd} + V_{wd} + V_{FRP} \tag{4}$$

where V_{cd} is the shear capacity of the concrete compression zone according to Eurocode 2 and Eurocode 8, V_{wd} is the shear carried by the web reinforcement through the truss mechanism according to Eurocode 8, and V_{FRP} is the FRPs contribution to shear capacity that can be written in the following form

$$V_{FRP} = 0.9\, \varepsilon_{f,e}\, E_f \rho_f\, b_w d \tag{5}$$

where d is the effective depth of cross section, b_w is the minimum width of cross section over the effective depth, ρ_f is the FRPs reinforcement ratio equal to ($2\, t_f/b_w$) for continuously bonded shear reinforcement of thickness t_f, E_f is the elastic modulus of FRPs in the principal fiber orientation and $\varepsilon_{f,e}$ is the design value of effective FRP strain, which is given by the following expression for fully wrapped or properly anchored FRPs (FIB-2001)

$$\varepsilon_{f,e} = \min\left[0.17\,\varepsilon_{fu}\left(\frac{f_{cm}^{2/3}}{E_f \cdot \rho_f}\right)^{0.3}, 0.006\right] \tag{6}$$

where f_{cm} is the mean value of the concrete compressive strength.

5.2 Proposed shear strength formulation

A new formulation published in recent studies (Tsonos 1999, 2002), predicts the beam-column joint ultimate shear strength and was used in the present study to predict the actual values of connection shear stress of the subassemblages F_1, $FRPF_1$ and $FRPS_1$. A summary of this formulation is presented in the following. The validity of the formulation was checked using test data for more than 120 exterior and interior beam-column subassemblages that were tested in the Structural Engineering Laboratory at the Aristotle University of Thessaloniki, as well as using data from similar experiments carried out in the United States.

Fig. 9(a) shows a reinforced concrete exterior beam-column joint for a moment resisting frame. The shear forces acting in the joint core are resisted: (i) partly by a diagonal compression strut and (ii) partly by a truss mechanism formed by horizontal and vertical reinforcement and concrete compression struts (Park and Paulay 1975). Both mechanisms depend on the core concrete strength. Thus, the ultimate concrete strength of the joint core under compression/tension controls the ultimate strength of the connection. After failure of the concrete, strength in the joint is limited by gradual crushing along the cross - diagonal cracks and especially along the potential failure planes (Fig. 9(a)).

For instance, consider the section I-I in the middle of the joint height (Fig. 9(a)). In this section, the flexural moment is almost zero. The forces acting in the concrete are shown in Fig. 9(b). T_i are the forces acting in the longitudinal column bars between the corner bars in the side faces of the column. These bars compress the joint core through equal and opposing directional forces. Each force acting in the joint core is analysed into two components along the X and Y axes (Fig. 9(b)). Thus, the vertically acting forces are

$$\underset{\substack{\downarrow \\ \text{compression strut}}}{D_{cy}} + \underset{\substack{\downarrow \\ \text{truss model}}}{(T_1 + \ldots + T_4 + D_{vy})} = D_{cy} + D_{sy} = V_{jv} \tag{7}$$

where V_{jv} is the vertical joint shear force (Eurocode 8).

The sum of the horizontally acting forces also gives the horizontal joint shear force as

$$D_{cx} + (D_{1x} + \ldots + D_{vx}) = V_{jh} \tag{8}$$

The normal vertical compressive stress σ and the shear stress τ uniformly distributed over the whole section are given by the Eqs. (9) and (10)

$$\sigma = \frac{D_{cy} + D_{sy}}{h'_c \times b'_c} = \frac{V_{jv}}{h'_c \times b'_c} \tag{9}$$

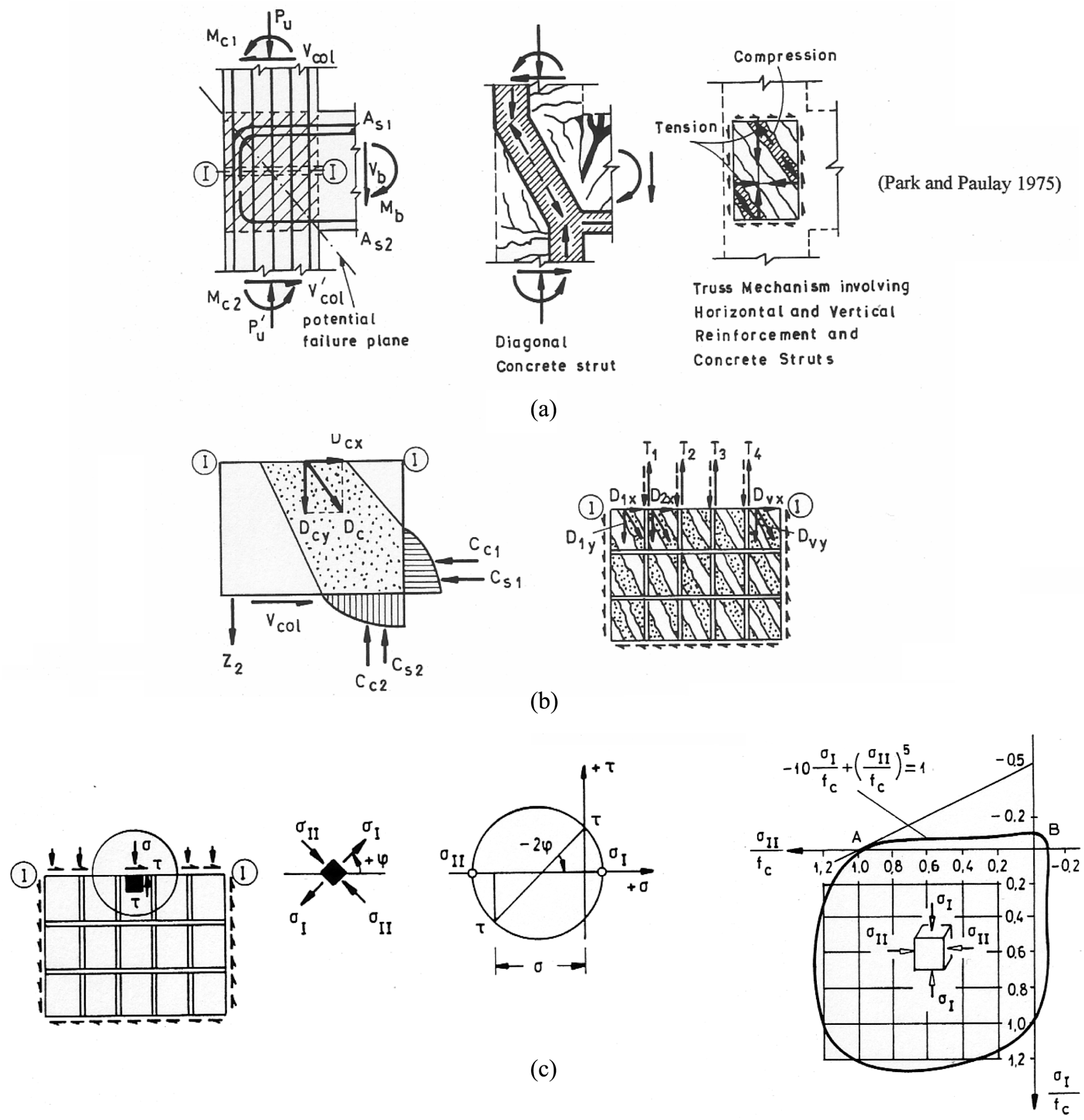

Fig. 9 (a) External beam-column connection and the two mechanisms of shear transfer (diagonal concrete strut and truss mechanism), (b) Forces acting in the joint core concrete through section I-I from the two mechanisms, (c) Stress state of element of the studied region and representation of concrete biaxial strength curve by a parabola of 5th degree

$$\tau = \frac{V_{jh}}{h_c' \times b_c'} \tag{10}$$

where h_c' and b_c' are the length and the width of the joint core respectively.

The relationship between the average normal compressive stress σ and the average shear stress τ are shown in Eq. (11)

$$\sigma = \frac{V_{jv}}{V_{jh}} \cdot \tau \tag{11}$$

where

$$\frac{V_{jv}}{V_{jh}} = \frac{h_b}{h_c} = \alpha \quad \text{(Eurocode 8)} \tag{12}$$

From Mohr's circle (Fig. 9(c))

$$\sigma_{\mathrm{I,\,II}} = \frac{\sigma}{2} \pm \frac{\sigma}{2}\sqrt{1 + \frac{4\tau^2}{\sigma^2}} \tag{13}$$

Eq. (14) was suggested for representing the concrete biaxial strength curve by a parabola of 5th degree (Tsonos 1999, Fig. 9(c))

$$-10\frac{\sigma_{\mathrm{I}}}{f_c} + \left(\frac{\sigma_{\mathrm{II}}}{f_c}\right)^5 = 1 \tag{14}$$

where f_c is the increased joint concrete compressive strength due to confining from steel hoops, which is given by the model of Scott *et al.* (1982) according to the equation

$$f_c = K \cdot f_c' \tag{15}$$

Confining a concrete member with an FRP-jacket is accomplished by orienting the fibers transverse to the longitudinal axis of the member. In this orientation, the hoop fibers are similar to conventional hoop reinforcing steel. Confinement results in an increase in the apparent strength of the concrete.

For a square or rectangular section wrapped with FRP-jacket and with corners rounded with a radius R the following equation gives the increased joint concrete compressive strength due to confining (Samaan *et al.* 1998, Triantafillou 2000)

$$f_c = f_c' + 6\left(2a\frac{t_f}{D}f_{fd,\,c}\right)^{0.7} \tag{16}$$

where

t_f : is the jacket thickness

$f_{fd,\,c} = 0.95\,f_{fk}$ (where f_{fk} is the characteristic value of the FRP tensile strength)

$a = 0.4 + 1.2(R/D)$ (where R/D is the ratio of the radius R to the equivalent diameter D). The values of a should be reduced to ($2/3\,a$) when the confining FRP-layers are more than 5. The equivalent diameter D is given by the expression $D = b^2/2h + h^2/2b$ where h, b are the section dimensions of the column or the beam-column joint.

Substituting Eqs. (11), (12) and (13) into Eq. (14) and using $\tau = \gamma\sqrt{f_c}$ gives the following expression

$$\left[\frac{\alpha\gamma}{2\sqrt{f_c}}\left(1 + \sqrt{1 + \frac{4}{\alpha^2}}\right)\right]^5 + \frac{5\alpha\gamma}{\sqrt{f_c}}\left(\sqrt{1 + \frac{4}{\alpha^2}} - 1\right) = 1 \tag{17}$$

Assume here that

$$x = \frac{\alpha\gamma}{2\sqrt{f_c}} \tag{18}$$

and

$$\psi = \frac{\alpha\gamma}{2\sqrt{f_c}}\sqrt{1 + \frac{4}{\alpha^2}} \tag{19}$$

Then expression (17) can be transformed into

$$(x + \psi)^5 + 10\psi - 10x = 1 \tag{20}$$

The solution of the system of Eqs. (18) to (20) gives the beam-column joint ultimate strength.

6. Comparison of predictions and experimental results

The proposed shear strength formulation can be used to predict the actual values of the connection shear stress of the subassemblages. Therefore, when the computed joint shear stress is greater or equal to the joint ultimate capacity $\gamma_{cal} \geq \gamma_{ult}$, the predicted actual value of connection shear stress will be near γ_{ult}, because the connection fails earlier than the beam(s). When the calculated joint shear stress is lower than the connection ultimate strength $\gamma_{cal} < \gamma_{ult}$, then the predicted actual value of connection shear stress will be near γ_{cal}, because the connection permits its adjacent beam(s) to yield.

In the original subassemblage F_1 both the columns and the beam-column joint are poorly detailed. Both these structural elements have been identified as critical structural elements, which appear to fail prematurely, thus performing as "weak links" in RC frames. In the retrofitted subassemblages $FRPF_1$ and $FRPS_1$ both the columns and the beam-column joints were strengthened and their strengthening schemes were designed according to the modern codes. Thus both these structural members do not perform as "weak links" of the RC frames.

Consequently, the question arises as to how a model which gives the ultimate strength of a reinforced concrete beam-column joint and which predicts the actual value of the joint shear stress can also be used for the prediction of the actual value of the column shear stress and, more generally, for the prediction of the actual values of shear forces and moments developed in the beam-column subassemblages of the present study during the tests. The answer can be found in

Table 3 Experimental and predicted values of the strength of subassemblages F_1, $FRPF_1$ and $FRPS_1$

Specimen	Joint aspect ratio $\alpha = \frac{h_b}{h_c}$	γ_{cal}	$\gamma_{\exp}$	γ_{ult}	Predicted shear strength τ_{pred} (1)	Observed shear strength $\tau_{\exp}$ (2)	$\mu = \frac{\tau_{pred}}{\tau_{\exp}}$
F_1	1.50	1.70	0.87	0.93	$0.93\sqrt{f_c}$	$0.87\sqrt{f_c}$	1.06
$FRPF_1$	1.50	0.94	0.85	1.67	$0.94\sqrt{f_c}$	$0.85\sqrt{f_c}$	1.10
$FRPS_1$	1.50	0.95	0.90	1.67	$0.95\sqrt{f_c}$	$0.90\sqrt{f_c}$	1.05

(1) For $\gamma_{cal} \geq \gamma_{ult}$, $\gamma_{pred} = \gamma_{ult}$ and $\tau_{pred} = \gamma_{ult}\sqrt{f_c}$ MPa
For $\gamma_{cal} < \gamma_{ult}$, $\gamma_{pred} = \gamma_{cal}$ and $\tau_{pred} = \gamma_{cal}\sqrt{f_c}$ MPa
An overstrength factor $a_0 = 1.25$ for the beam steel is included in the computations of joint shear stress $\tau_{cal} = \gamma_{cal}\sqrt{f_c}$ MPa
(2) $\tau_{\exp} = \gamma_{\exp}\sqrt{f_c}$ MPa

Paulay and Priestley (1992), who clearly demonstrated that the shear forces acting in the beam-column joints are significantly higher than those acting in their adjacent columns. Thus the joints fail earlier than the columns during a strong earthquake motion.

Consequently, a model predicting the actual value of the joint shear stress could also predict the shear stress of the adjacent columns of a subassemblage and could also predict the actual values of shear forces and moments resisted by the subassemblages of the present study during the tests.

The comparison between experimental and predicted results by the preceding methodology for all the specimens in the present study is shown in Table 3. A particularly close correlation can be observed.

It is worth mentioning here that the prediction of the actual values of connection shear stress during an earthquake also involves the prediction of the actual values of the subassemblages' M_R ratio with the same degree of accuracy.

7. Conclusions

Based on the results described in this paper, the following conclusions can be drawn.

1. Original specimen F_1 representing an existing beam-column subassemblage designed to older codes, performed poorly under reversed cyclic lateral deformations. The connection of this subassemblage exhibited premature shear failure during the early stages of cyclic loading, and damage to the subassemblage was concentrated in the joint region.
2. The retest of the failed beam-column subassemblage, repaired and strengthened with fiber carbon/epoxy jacketing, showed that the employed repair and strengthening technique was effective in transforming the brittle joint shear failure mode of original specimen F_1 into a more ductile failure mode with the development of flexural hinge into the beam. Damage of the strengthened specimen $FRPF_1$ was concentrated in both the beam's critical region and in the joint area.
3. The effectiveness of the high-strength fiber jacket system was demonstrated both in a post-earthquake and a pre-earthquake retrofitting case of reinforced concrete columns and beam column joints.
4. A new formulation which predicts the beam-column joint ultimate shear strength was used to predict the actual values of the connection shear stress of all the subassemblages investigated in the present study. In all cases the observed capacity was predicted to within approximately 10 percent of that computed using the joint shear strength formulation (Table 3).

Acknowledgements

The experimental part of this research was sponsored by the Earthquake Planning and Protection Organization (E.P.P.O.). The author gratefully acknowledges the support provided by the sponsor.

References

ACI-ASCE Committee 352-2002. “Recommendations for design of beam-column joints in monolithic reinforced

concrete structures (ACI 352R-02)", *American Concrete Institute*, 37pp.
ACI Committee 440 (1996), "State of the art report on fiber reinforced plastic reinforcement for concrete structures (ACI 440R-96)", *American Concrete Institute*, Detroit, 68pp.
Antonopoulos, C. and Triantafillou, T. (2003), "Experimental investigation of FRP-strengthened RC beam-column joints", *J. Compos. Const.,* **7**(1), 39-49.
Dritsos, S. (1997), "Jacket retrofitting of reinforced concrete columns", *J. Const. Repairs*, **11**(4), 35-40.
Dritsos, S. (2001), "Repair and strengthening of reinforced concrete structures", Patras, 309pp. (in Greek).
Dritsos, S. (2005), "Seismic retrofit of buildings a greek perspective", *Bulletin of New Zealand Society for Earthq. Eng.*, **38**(3), 165-181.
Eurocode No 2 (2003), "Design of concrete structures-Part 1-1: General rules and rules of buildings, prEN 1992-1-1: 2003E", *Commission of the European Communities.*
Eurocode No 8 (2004), "Design of structures for earthquake resistance, Part I: General rules, seismic actions and rules for buildings, EN 1998-1:2004E", *Commission of European Communities.*
FIB (CEB-FIP), (2001), "Externally bonded FRP reinforcement for RC structures", Technical Report, Bulletin 14, 131pp.
Greek Code for the Design of Reinforced Concrete Structures.(2000), (C.D.C.S.-2000), *Ministry of Environment, Land Planning and Public Works, General Secretariat of Public Works*, Athens, 497pp.
Hakuto, S., Park, R. and Tanaka, H. (2000), "Seismic load tests on interior and exterior beam-column joints with substandard reinforcing details", *ACI Struct. J.*, **97**(1), 11-25.
Ilki, A. and Kumbasar, N. (2002), "Behavior of damaged and undamaged concrete strengthened by carbon fiber composite sheets", *Struct. Eng. Mech., An Int. J.*, **13**(1), 75-90.
Karayannis, C., Chalioris, C. and Sideris, K. (1998), "Effectiveness of RC beam-column connection repair using epoxy resin injections", *J. Earthq. Eng.*, **2**(2), 217-240.
Park, R. and Paulay, T. (1975), "Reinforced concrete structures", *John Wiley Publications*, New York, 769pp.
Paulay, T. and Priestley, M.J.N. (1992), "Seismic Design of Reinforced Concrete and Masonry Buildings", John Wiley & Sons.
Penelis, G.G. and Kappos, J.A. (1997), "Earthquake-resistant concrete structures", *E & FN SPON, An Imprint of Chapman & Hall*, 572pp.
Priestley, M.J.N., Seible, F. and Calvi, G.M. (1996), "Seismic design and retrofit of bridges", *A Wiley-Interscience Publication, John Wiley & Sons Inc.*, New York, 687pp.
Samaan, M., Mirmiran, A. and Shahawy, M. (1998), "Model of concrete confined by fiber composites", *J. Struct. Eng.*, ASCE, **124**(9), 1025-1031.
Scott, B.D., Park, R. and Priestley, M.J.N. (1982), "Stress-strain behavior of concrete confined by overlapping hoops at low and high strain rates", *ACI J., Proc.*, **79**(1), 13-27.
Thermou, G.E. and Elnashai, A.S. (2006), "Seismic retrofit schemes for R/C structures and local-global consequences", *Progess in Struct. Eng. Mater.*, **8**(1), 1-15.
Triantafillou, T. (2000), "Design of reinforced concrete and masonry structures strengthened with FRP", *Strengthening of Reinforced Concrete Structures with FRP, Meeting Organized by the Technical Chamber of Greece, Athens (in Greek).*
Tsonos, A.G. (1999), "Lateral load response of strengthened reinforced concrete beam-to-column joints", *ACI Struct. J. Proc.*, **96**(1), 46-56.
Tsonos, A.G. and Stylianides, K. (2002), "Seismic retrofit of beam-to-column joints with high-strength fiber-jackets", *J. Euro. Assoc. Earthq. Eng.,* No. 2, 56-72.
Tsonos, A.G. (2002), "Seismic repair of reinforced concrete beam-column subassemblages of modern structures by epoxy injection technique", *Struct. Eng. Mech., An Int. J.*, **14**(5), 543-563.
Tsonos, A.G. (2003), "Effectiveness of CFRP - Jackets and RC - Jackets in post-earthquake and pre-earthquake retrofitting of beam-column subassemblages", *Final Report on Research Conducted Under Grant No. 100/11-10-2000 from the Earthquake Planning and Protection Organization (E.P.P.O.)*, 167pp. (in Greek).